EFFECT OF SECRETOME OF SKELETAL MUSCLE ON ISLET DIFFERENTIATION & FUNCTIONALITY

CHAPTER 4

Chapter 4: Effect of secretome of skeletal muscle on islet differentiation & functionality

4.1 Introduction

Glucose homeostasis is regulated by the pancreatic β cells in communication with various other organs. One such important communication is with skeletal muscle, which plays a vital role in glucose metabolism in the postprandial state, and impaired action on skeletal muscle leads to the pathological condition of insulin resistance. The importance of skeletal muscle in insulin resistance points toward its traditional role as an insulin-dependent organ that functions in regulating glucose homeostasis. Thus, skeletal muscle-islet crosstalk plays a key determinant in maintaining normal physiological and biological functions. The exchange of inter-cell interactions by autocrine, paracrine, or endocrine functions plays a primary role in divergent pathophysiological conditions. Any derangement in such a communication initiates a cascade of metabolic catastrophes such as diabetes mellitus (DeFronzo and Tripathy 2009) (Castillo-Armengol, Fajas et al. 2019). Pancreatic β cell function, regulation, and mass are important aspects of understanding diabetes. Type 1 diabetes mellitus is characterized by auto-destruction of pancreatic β cells (Bluestone, Herold et al. 2010). Whereas Type 2 diabetes mellitus is characterized by a series of metabolic disturbances like insulin resistance which are often an outcome of a deficit of regular physical exercise and a sedentary lifestyle (Cerf 2013) (Bouzakri, Plomgaard et al. 2011) (Pedersen 2009).

Skeletal muscle apart from being a locomotory organ has also been identified as secretory in nature. Various distal regulatory effects of skeletal muscle are mediated by small molecules, proteins, peptides, etc which comprise the skeletal muscle secretome. Myokines are the key mediators of skeletal muscle as a part of the interorgan crosstalk network which mediates communication between pancreas, the liver, adipose tissue, the brain, kidney, etc.

Numerous myokines have now been identified which exhibit regulatory effects on various other organs including β cells (Eckardt, Görgens et al. 2014) (Pedersen and Febbraio 2012) E.g., Interleukin 6 (IL6) has been an extensively studied prototype of a myokine. IL6 has been well documented for its effect on β cells. As a myokine, it protects against the detrimental effects of

type 2 diabetes (Pedersen and Febbraio 2012). Reports suggest that the secretome profile of skeletal muscle changes with various stimuli like hyperinsulinemia, hyperglycemia, inflammation, etc. Differential secretion of myokines by normally sensitive or insulin-resistant myotubes affects β cells positively and detrimentally affects their survival and functionality (Bouzakri, Plomgaard et al. 2011) (Ciaraldi, Ryan et al. 2016). Thus, the effect of skeletal muscle secretome is widely studied on islet functionality but remains unexplored on islet neogenesis or differentiation.

The present chapter focuses on communication between skeletal muscle and pancreatic islets under normal and insulin resistant conditions, not only in terms of islet functionality but also islet neogenesis which is yet to be properly defined. This report will widen our knowledge of skeletal muscle therapeutics along with its restoring capacities on islet differentiation and functionality

4.2Material and Methods and Experimental Design

4.2.1 Cell culture

C2C12 cell line was maintained at 37 °C in 5% CO2 in DMEM high glucose (Gibco#12100-046) with 10% FBS (Gibco#10270-106) and 1.0% of penicillin-streptomycin (PS) (Gibco#15140-122). Differentiation of C2C12 myoblast into myotubes was brought by supplementation with DMEM high glucose with 2% FBS and 1.0% PS from day 0 to day 5 and insulin resistance was created by treating one group of cells with 1 nM TNFα for 24 h.

Mouse pancreatic resident endocrine progenitors were earlier isolated by digestion of mouse pancreas and cryopreserved as described previously (Bhardwaj, Vakani et al. 2022) (Dadheech, Srivastava et al. 2015) (Srivastava, Dadheech et al. 2018) (Srivastava, Dadheech et al. 2018) and were propagated in DMEM high glucose (Gibco#12100-046) at 37 °C in 5% CO2 with 10% FBS (Gibco#10270-106) and 1.0% of penicillin-streptomycin (Gibco#15140-122).

4.2.2 May-grunwald giemsa staining

C2C12 myoblast and Post differentiation myotubes were fixed with 4% PFA after washing with PBS. After removing PFA, cells were stained with 1 ml May grunwald working solution for 5 min and 1 ml Giemsa working solution for 10 mins. After washing with buffered water (diluted phosphate buffer), and allowing to dry at room temperature, cells were microscopically observed (Nikon Instruments Inc.).

4.2.3 Conditioned media (CM) preparation from C2C12 myotubes

Control and insulin resistant C2C12 myotubes were supplemented with serum free KnockOut^{TM} DMEM (Gibco#10829-018) with and without TNFα respectively post 5 days differentiation and propagated at 37 °C in 5% CO2. After 24 h of incubation, media was collected centrifuged at 4000 rpm for 30 min. Supernatant was filtered through 0.2mm filter and stored at -80 ^{0}C after until further experiment use.

4.2.4 LCMS of Conditioned media (CM) of C2C12 myotubes

Secretome LCMS analysis was performed on Q-Exactive Plus Biopharma-High Resolution Orbitrap Liquid Chromatograph Mass Spectrometer (Thermo Fischer Scientific Ptv. Ltd) (Facility hired at SAIF, IIT Bombay, India) The Chromatographic separation was performed on Analytical Column: PepMap RSLC C18 2um, 100A x 50 cm, Pre-column: Acclaim PepMap 100, 100um x 2cm nanoviper. The mobile Phase used was: solvent A: 0.1% Formic acid in milliq water, solvent B: 80:20 (Acetonitrile:milliq water) + 0.1% Formic acid. Data acquisitions and mass spectrometric data analysis software used was Thermo Proteome Discoverer 2.2. The abundance and classification of proteins were analysed using Panther database (Thomas, Campbell et al. 2003) (Fig 4.1).

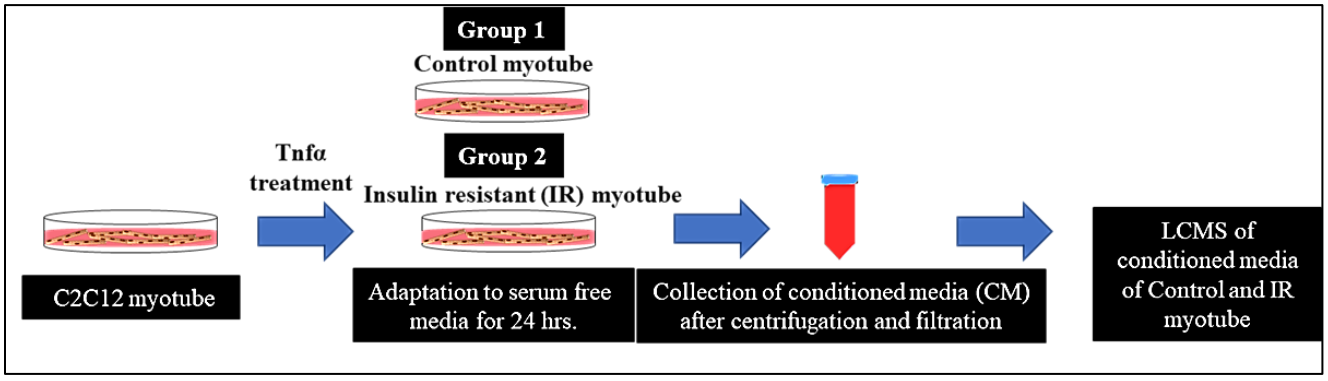

Figure 4.1 *In vitro* Plan of work insulin resistant model generation and secretome collection

4.2.5 Differentiation of ILCCs from PREPs under the effect of C2C12 myotubes secretome

ILCCs were differentiated from the PREPs with differentiation media which contains serum-free KnockOut^{TM} DMEM (Gibco#10829-018) media supplemented with 1% BSA, 1X glutamax, insulin (5 µg/ml), transferrin (5 µg/ml), and selenite (5 ng/ml) cocktail, 1X Zinc acetate, 1.0% of penicillin-streptomycin and swertisin (15 µg/ml) as differentiating agent, as previously reported

(Bhardwaj, Vakani et al. 2022) (Dadheech, Soni et al. 2013) (Dadheech, Srivastava et al. 2015) (Srivastava, Dadheech et al. 2018). PREPs were subjected to fifty percent of control and insulin resistant (IR) C2C12 myotubes CM diluted with differentiation media till the termination of islet differentiation in a 4 day protocol (Fig 4.2).

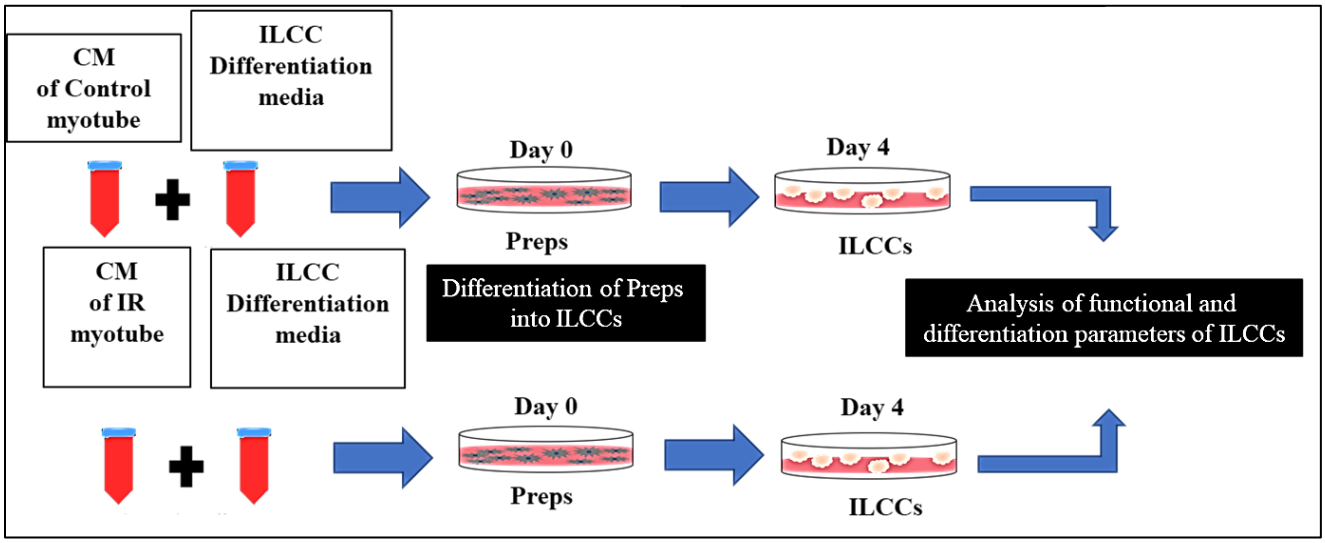

Figure 4.2 *In vitro* Plan of work of differentiation of PREP into ILCCs.

4.2.6 Yield, Morphometry analysis and DTZ staining

ILCCs were treated with control and IR C2C12 myotubes CM and were observed in a phase-contrast microscope (Nikon Instruments Inc.). After centrifuging, washing with PBS and staining with DTZ solution they were photographed. Total yield was evaluated and morphometry analysis was performed with Image J software.

4.2.7 Immunocytochemistry

C2C12 myoblast and Post differentiation myotubes were washed with PBS and fixed in 4% PFA on ice for 10 min. After permeabilization with 0.1% triton X-100 for 5 min at 4°C, cells were subjected to blocking buffer for 1 hr at room temperature and then incubated with αSMA primary antibody (Sigma#F3777) overnight at 4 °C. Cells were viewed under a fluorescence microscope (Nikon Instruments Inc.) after counterstaining with DAPI.

Differentiated ILCCs were collected, washed with PBS and centrifuged before fixing in chilled absolute methanol for 10 min. ILCCs were permeabilized with 0.1% triton X-100 for 5 min at 4°C. ILCCs were then subjected to blocking buffer (2% BSA) for 1 hr at room temperature followed by

incubation in C-peptide (CST#4593), glucagon (Sigma#G2654) primary antibodies overnight at 4 °C. ILCCs were washed and then incubated with respective secondary antibodies Anti-Rabbit-IgG-FITC (Sigma#F9887) and Anti-Mouse-IgG-CF555 (Sigma#SAB4600299) for 1 hour and then counterstained with DAPI, washed with PBS, mounted with coverslips. ILCCs were observed under a confocal microscope (Zeiss LSM 710).

4.2.8 DCFDA staining

ILCCs were centrifuged and washed with PBS. ILCCs were resuspended in 990 µl of PBS and 10 µl of 10 mg/ml of DCFDA (2',7'–dichlorofluoresceindiacetate) dye was then added and incubated at room temperature for 20 min. ILCCs were then incubated with DAPI for 10 min. ILCCs were centrifuged and washed with PBS, then observed under a phase contrast fluorescent microscope (Nikon Instruments Inc.).

4.2.9 FDA/PI staining

ILCCs were centrifuged and washed with PBS. Then, ILCCs were resuspended in PBS and FDA (0.5 mg/mL) and PI (2 mg/mL) were added to the ILCCs. After incubation at room temperature for 30 min, ILCCs were observed under a phase contrast fluorescent microscope (Nikon Instruments Inc.).

4.2.10 Annexin/PI staining

ILCCs were centrifuged and resuspended in PBS and Annexin (5 µg/mL) and PI (2 mg/mL) were added to the ILCCs. ILCCs were viewed under a phase contrast fluorescent microscope (Nikon Instruments Inc.) after incubation at room temperature for 30 min.

4.2.11 RNA extraction and Gene expression

Total RNA from myoblast, control and IR myotubes were isolated using in TRIZOL™ reagent (Invitrogen#15596018) and cDNA was synthesized using High-Capacity cDNA Reverse Transcription Kit (Applied Biosystems#4368814) as per the manufacturer's protocol. All the target genes from *MyoG, Insr, Irs1, Glut4, IL6, IL13, IL15, IL10, CXCL1, CX3CL, FGF21* were amplified on ABI-7500™, Applied Biosystems qPCR system using SYBR premix Ex Taq II (Takara#RR820A). *Actb* was used as the internal control. The primer sequence is summarized in Table (Refer Appendix).

4.2.12 Protein extraction and western blotting

ILCCs were centrifuged, washed, harvested and kept on ice. C2C12 control and IR myotubes were harvested after 15 min of 100nM insulin treatment. ILCCs, myotubes and myoblast were lysed in Laemmli lysis buffer. Protein concentration was estimated by Bradford's method and 15 µg of protein were resolved and transferred to nitrocellulose membrane. Blots were then kept in blocking buffer for an hour.

Blots were then probed with Desmin(Sigma#8281), Insulin Receptor β(BD#611277), IRS-1 (CST#2381),Akt(CST#4691S),pAkt(CST#4060P),Caspase-3(Invitrogen#PA1-29157),Parp1 (Santacruz#SC1561),HNF3B(DSHB#4C7),NGN3(Sigma#SAB1306585),NeuroD1(CST#4373),Nestin(Sigma#N5413),PAX4(Sigma#AV32064),Nkx6.1(DSHB#F64A6B4),PDX1(BD#554655),GLUT-2(Sigma #SAB1303865),MAF-A (Sigma #SAB2105099) and Beta-Actin (BD#612657) primary antibodies and kept overnight at 4 °C.

Blots were incubated with respective HRP- conjugated secondary antibodies for 1 h at RT after washing with PBST and PBS. Proteins bands were visualized by means of enhanced chemiluminescence (ECL) reagent (Bio-Rad) and images were taken on Alliance 4.7 UVI Tec Chemidoc (Uvitech, Cambridge) gel documentation system. Densitometric analysis was performed by Image J software.

4.2.13 Statistical analysis

Data is represented as Mean ± SEM and was evaluated by the Student's t-test or ANOVA by Graphpad prism 7 or Microsoft excel 2016.

4.3RESULTS

We investigated the indirect crosstalk between muscle and pancreatic islet by studying the trophic effects. We selected the shortest route of islet differentiation from pancreatic resident endocrine progenitors to understand influence of the secretome of insulin resistant myotubes on islet neogenesis, integrity and functionality.

4.3.1 Formation and confirmation of C2C12 myogenic differentiation into myotubes

C2C12 myoblasts undergo *in vitro* myogenesis to yield multinucleated myotubes. Myoblast were mononuclear in the growth phase at day 0. When the myoblasts were nearly confluent, they began

to fuse 2–3 days after the induction of differentiation. Myotube density was observed to be sharply increased from day 3 to form multinucleated myotubes which were formed by day 5 and observed at day 7 till end of the differentiation protocol.

To establish myotube model, we stained the cells with may-grunwald giemsa staining which clearly showed mono and post mitotic multinucleasted elongated myotubes (Fig 4.3).

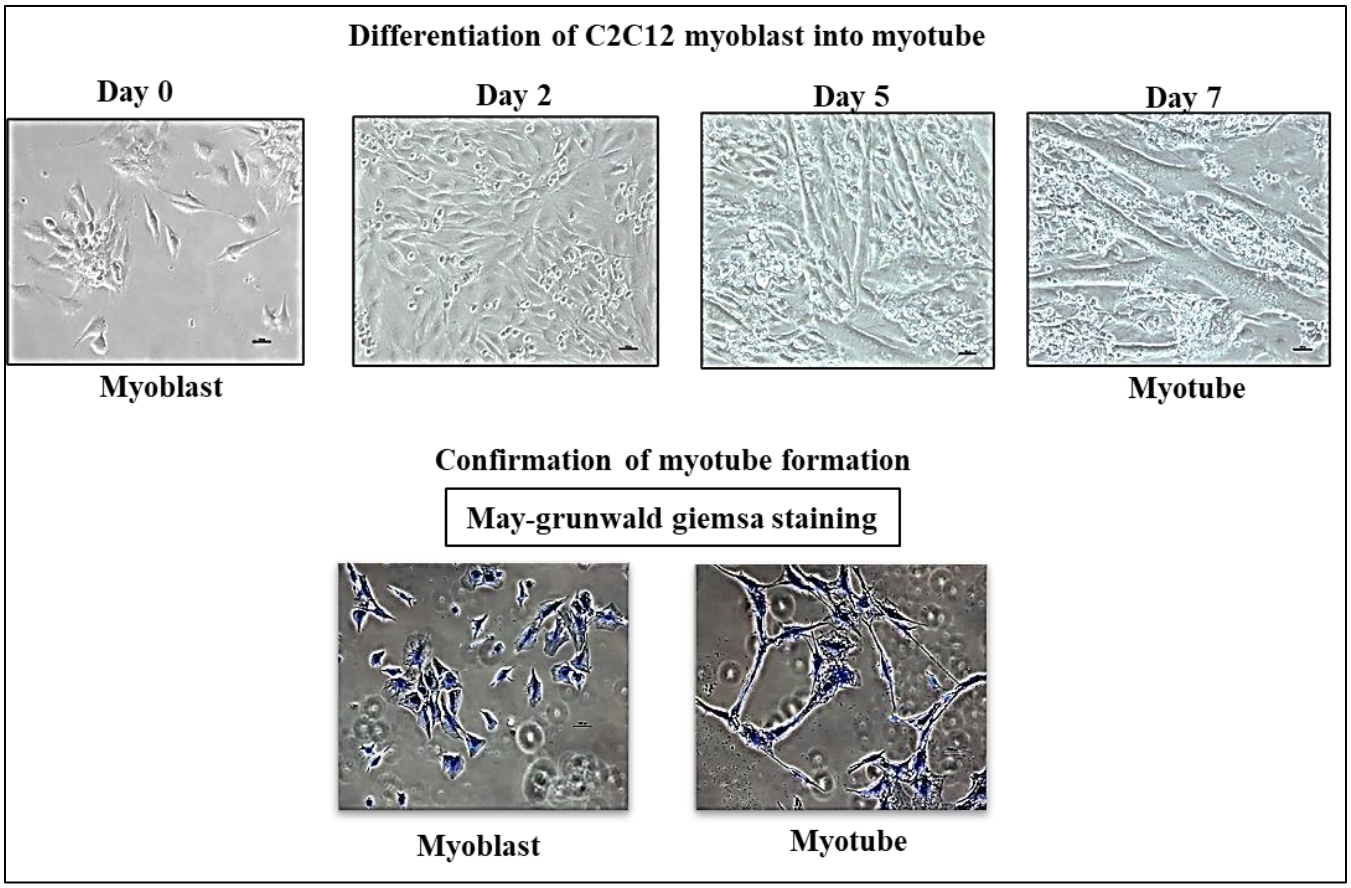

Figure 4.3 Differentiation of C2C12 myoblast into myotubes. Day wise maturation of myoblast into myotube. Visualization of myotube formation by May-grunwald giemsa staining

Myoblasts undergo remodeling to differentiate into mature myotubes with increased expression of myogenic genes (Maglara, Vasilaki et al. 2003). So important myogenic markers like myogenin, a marker for the entry of myoblasts into the differentiation pathway (Andrés and Walsh 1996) and desmin, the chief intermediate filament protein of myocyte were evaluated (Mermelstein, Amaral et al. 2005). Gene and protein expression of myogenin and desmin respectively were significantly

upregulated in myotube compared to myoblast. We also confirmed higher expression of αSMA (Alpha-smooth muscle actin) in myotubes, which is a major component of the cytoskeletal structural network (Corvino, Cerqua et al. 2021). Immunofluorescence of FITC-labeled αSMA clearly distinguish myoblast and myotube (Fig 4.4)

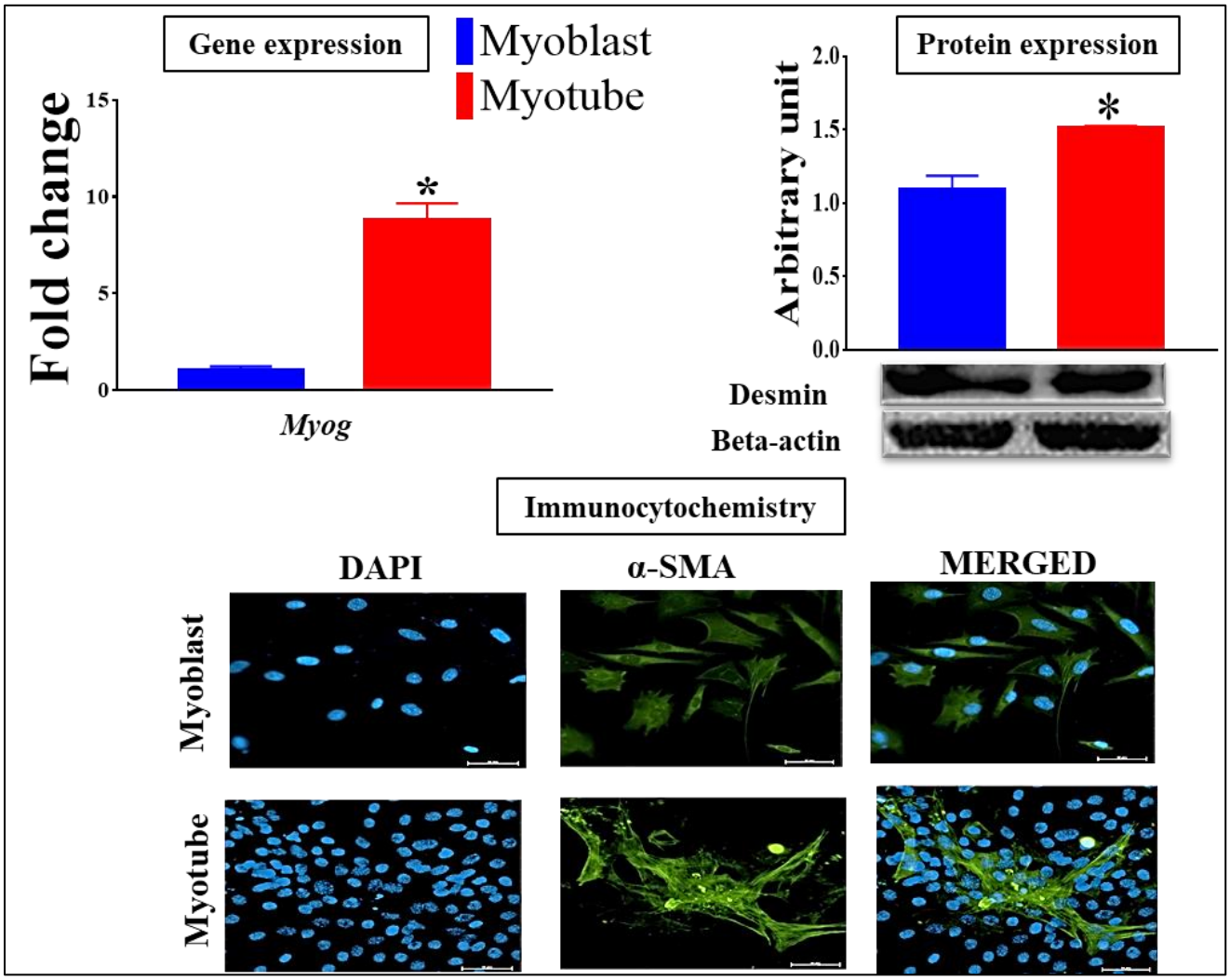

Figure 4.4 Confirmation of C2C12 myoblast into myotubes. Confirmation by gene expression of myogenin (Data is expressed as Fold change ± S.E.M. N=3), protein expression of desmin (Densitometric analysis was done normalized to beta-actin and data expressed as arbitrary unit± S.E.M. N=3). Significance is expressed as p-value *<0.05 and immunocytochemistry of α-SMA was performed (magnification 20x).

4.3.2 TNF-α induced insulin resistance in C2C12 myotubes

In order to generate *in vitro* insulin resistant muscle model**,** myotubes were subjected to TNFα treatment (del Aguila, Claffey et al. 1999). We confirmed the state of insulin resistance by examining the expression of key insulin signaling proteins. Gene expression of *Insr*, *Irs1* and *Glut4* were significantly downregulated in insulin resistant (IR) myotube (Fig 4.5). Protein expression of IR, IRS1 and pAkt/Akt ratio was also reduced in IR group (Fig 4.6).

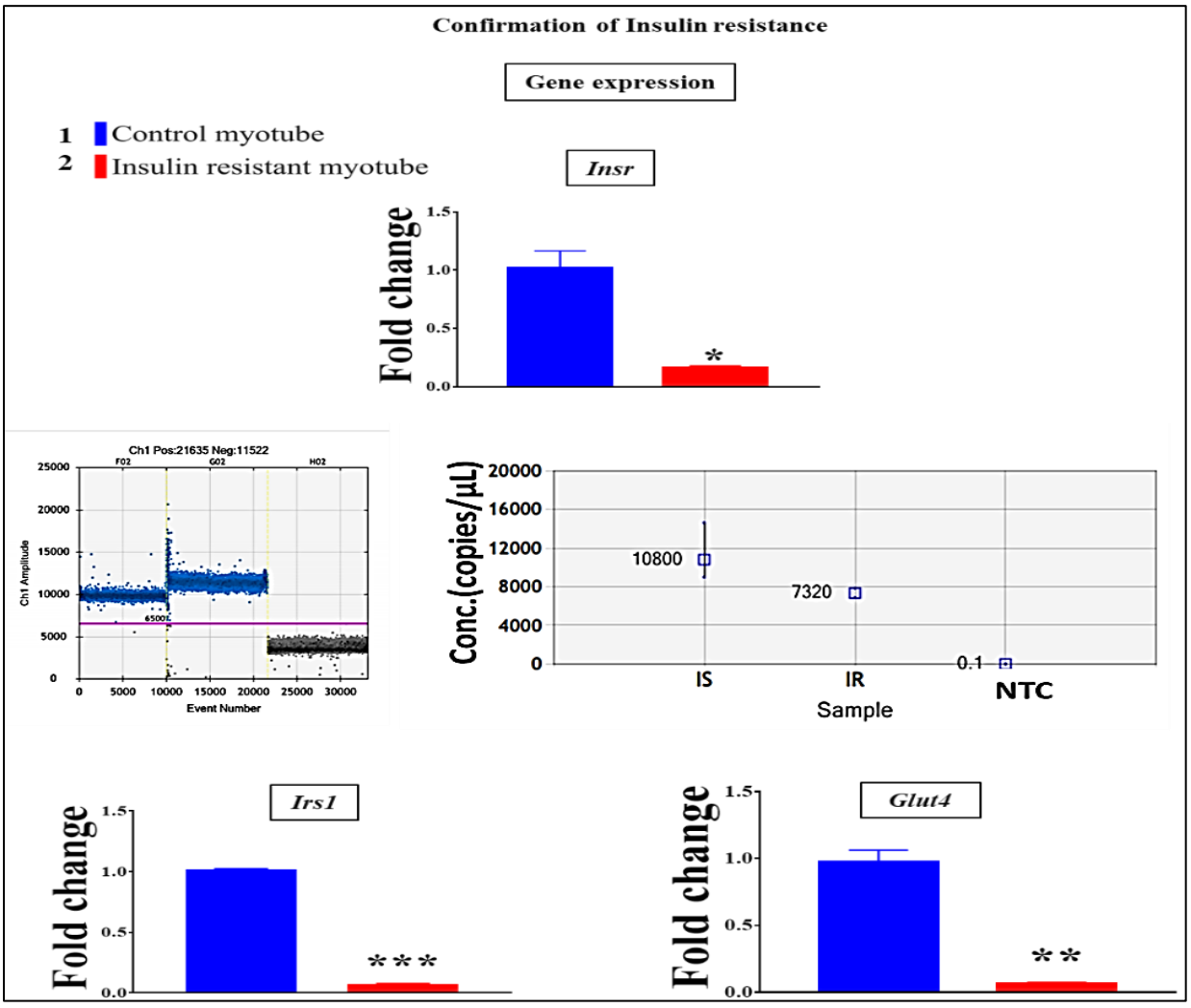

Figure 4.5 Confirmation of insulin resistance in C2C12 myotube Myotubes were treated with TNF-α to make *in vitro* insulin resistant model and confirmation of insulin resistant condition was done by Gene expression of Insr (Expression of *Insr* was evaluated both by RT-PCR and

dd-PCR), *Irs1*, *Glut4* was done (Data is expressed as Fold change ± S.E.M. N=3). Significance is expressed as p-value *<0.05, ** <0.01, * <0.001**

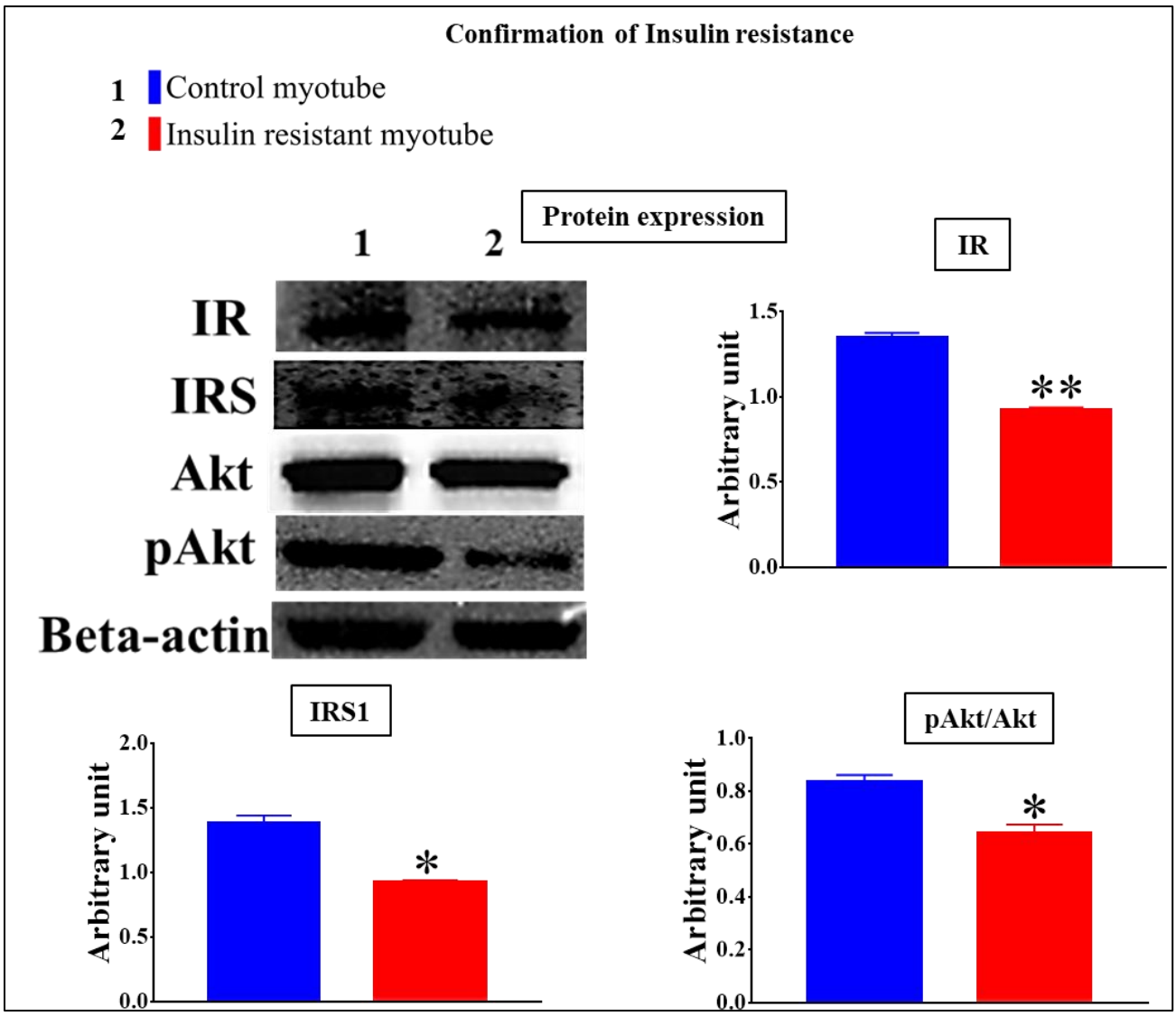

Figure 4.6 Confirmation of insulin resistance in C2C12 myotube Myotubes were treated with TNF-α to make *in vitro* insulin resistant model and confirmation of insulin resistant condition was done by Protein expression of IR, IRS1, pAkt/Akt key insulin signaling proteins (Densitometric analysis was done normalized to beta-actin and expressed as arbitrary unit± S.E.M. N=3). Significance is expressed as p-value *<0.05, ** <0.01

4.3.3 Insulin resistance affects the myokine profiling from C2C12 myotubes

Distal regulatory factors like myokines are secreted by muscle. To expand our understanding of the secretion profile of myokines under insulin resistant condition, we determined gene expressions of various myokines which are important trophic factors for muscle and islets. *IL6, IL13, IL15, IL10, CX3CL1, CXCL1, FGF21* myokine levels were evaluated by gene expression (Fig 4.7). *IL6, CX3CL1, FGF21* were significantly upregulated and rest were downregulated in insulin resistant (IR) myotube compared to control. This compelling evidence reinstates that myokines panel is detrimentally affected by insulin resistance.

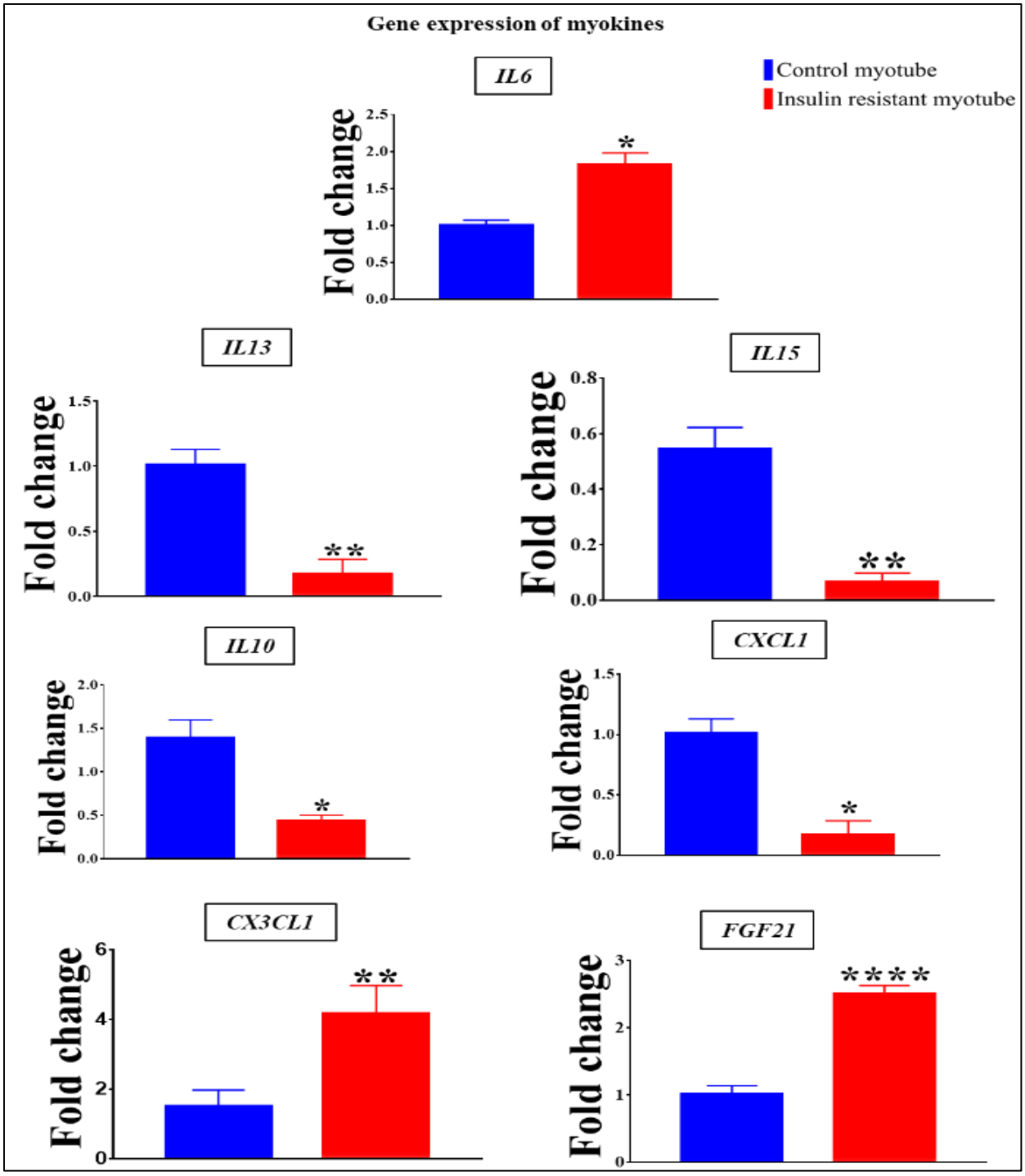

Figure 4.7 Myokine gene expression in C2C12 myotube under insulin resistance. Differential gene expression of *IL6, IL13, IL15, IL10, CX3CL1, CXCL1, FGF21* myokines were performed

in control and IR C2C12 myotubes. Data is expressed as Fold change ± S.E.M. N=3. Significance is expressed as p-value *<0.05, <0.01, **** <0.0001.**

4.3.4 Protein characterization from the secretome of control and IR C2C12 myotube

Secretory factors from the secretome of control and IR C2C12 myotube were analysed from conditioned media by LCMS. A striking difference was observed in the chromatogram for both the secretome samples. A different pattern of peaks was detected at varying retention times. The highest chromatographic peak was observed at 34.83 min and 47.11 min in conditioned media of control and IR C2C12 myotube respectively (Fig 4.8).

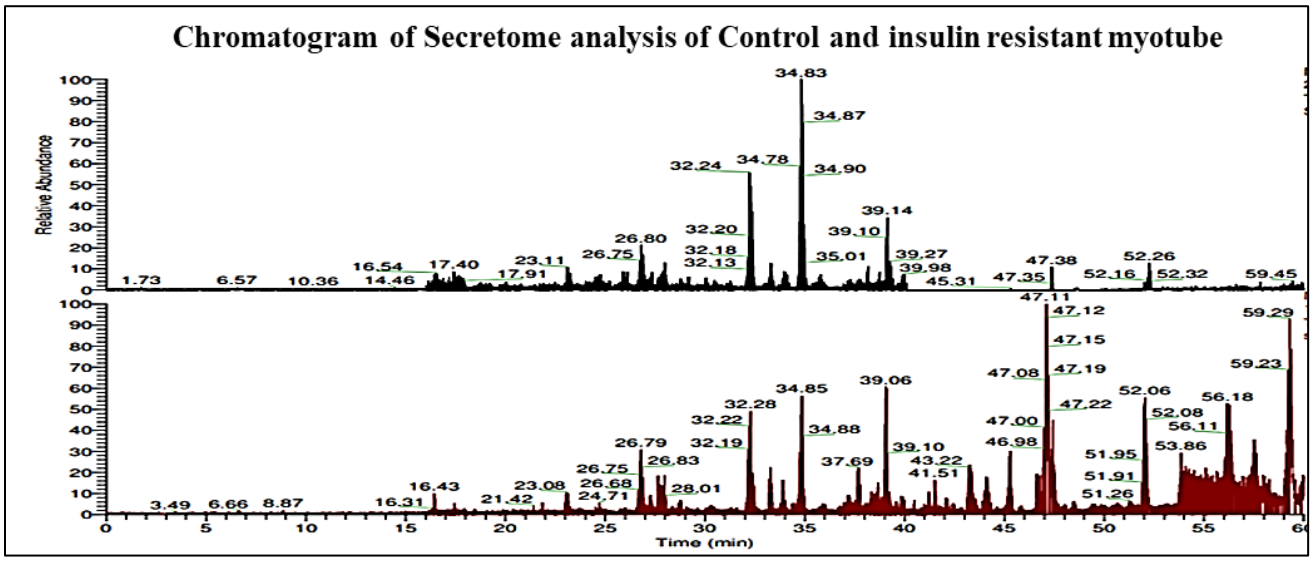

Figure 4.8 Characterization of differentially regulated proteins from secretomes. Chromatogram of secretomes of C2C12 myotube from control and IR groups.

The majority of the proteins were underexpressed in IR myotube secretome compared to control which had a notable correlation with differential expression and abundance of proteins. We categorized these proteins using Panther database (Thomas, Campbell et al. 2003) which uses gene ontology analysis for classification into molecular function, biological process, cellular component, protein class, and pathway.

When analyzed for molecular function, most of the proteins were categorized under molecular transducer activity (GO:0060089) and binding (GO:0005488).

Biological processes categorized proteins into the response to stimulus (GO:0050896), signaling (GO:0023052), immune system process (GO:0002376), cellular process (GO:0009987), multicellular organismal process (GO:0032501), metabolic process (GO:0008152) biological regulation (GO:0065007).

Cellular anatomical entity (GO:0110165), Protein-containing complex (GO:0032991) and intracellular (GO:0005622) belonged to cellular component class.

Proteins were categorized under protein classes as scaffold/adaptor protein (PC00226).

For pathway analysis proteins were classified into T cell activation (P00053) (Fig 4.9). These differential classifications of proteins reinforce the fact that there is an appreciable difference in the secretome which is a consequence of insulin resistance environment subjected to C2C12 myotubes.

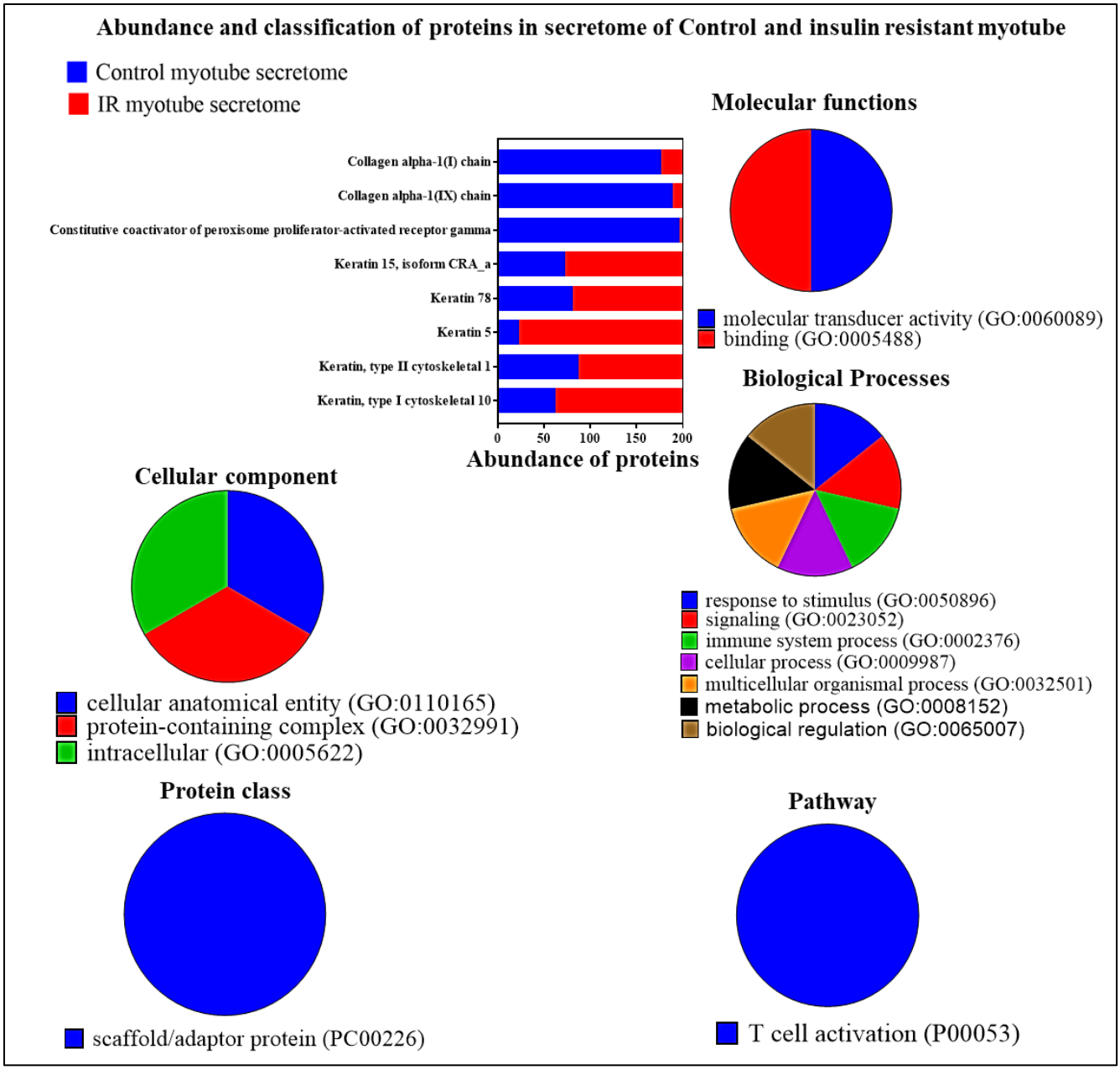

Figure 4.9 Characterization of differentially regulated proteins from secretomes. Graph showing Abundance and Classification of proteins present in secretomes of C2C12 myotubes from control and IR groups

4.3.5 ILCCs from PREPs demonstrates compromised functional and phenotypic characterization under IR C2C12 myotube secretome

Owing to the fundamental interest in analyzing islet differentiation under the effect of secretory products of myotubes, PREPs were allowed to differentiate with control and IR C2C12 myotube secretome in a 4 day protocol supplemented with islet differentiation media combined with secretomes (Fig 4.10). Cluster formation was monitored microscopically for 4 days and more participation of PREPs, maximum cell aggregation, and zone of activation was observed in ILCCs under the effect of control C2C12 myotube secretome in contrast to IR, suggesting effective endocrine reprogramming.

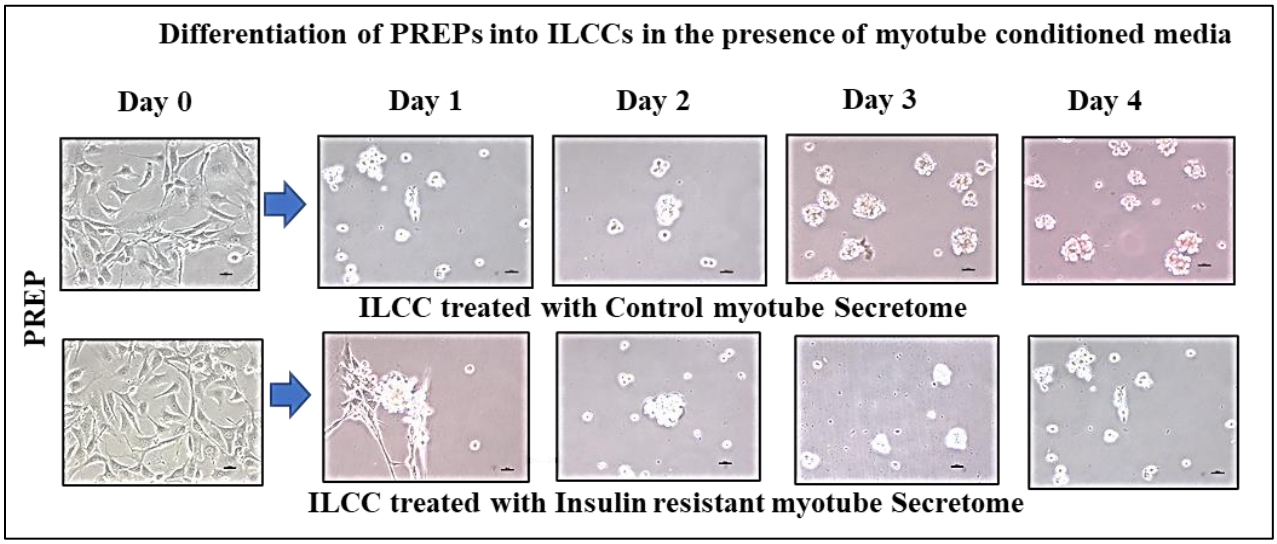

Figure 4.10 Representative images of temporal differentiation of ILCC from day 0 to day 4. PREPs were subjected to control and IR secretomes of C2C12 myotubes and ILCCs were differentiated.

Further in insulin positive cells, by DTZ staining, a brighter red colour was observed, in ILCCs under the effect of control C2C12 myotube compared to IR. To monitor the maturation of ILCCs we immunostained the clusters with C peptide and glucagon (Fig 4.12). It was noteworthy to observe intense red and green staining in ILCCs under the effect of control C2C12 myotube secretome as contrast to IR confirming more insulin positive content. The critical correlation of immunocytochemistry of ILCCs pointed towards incomplete and immature functional differentiation under IR C2C12 myotube secretome. We observed decreased yield in the IR group.

The population of ILCCs was heterogeneous with most ILCCs falling in 100-250 um range in control compared to IR group These results offered compelling evidence of the inadequacy of functional maturation of ILCCs when subjected to IR C2C12 myotube secretome (Fig 4.11).

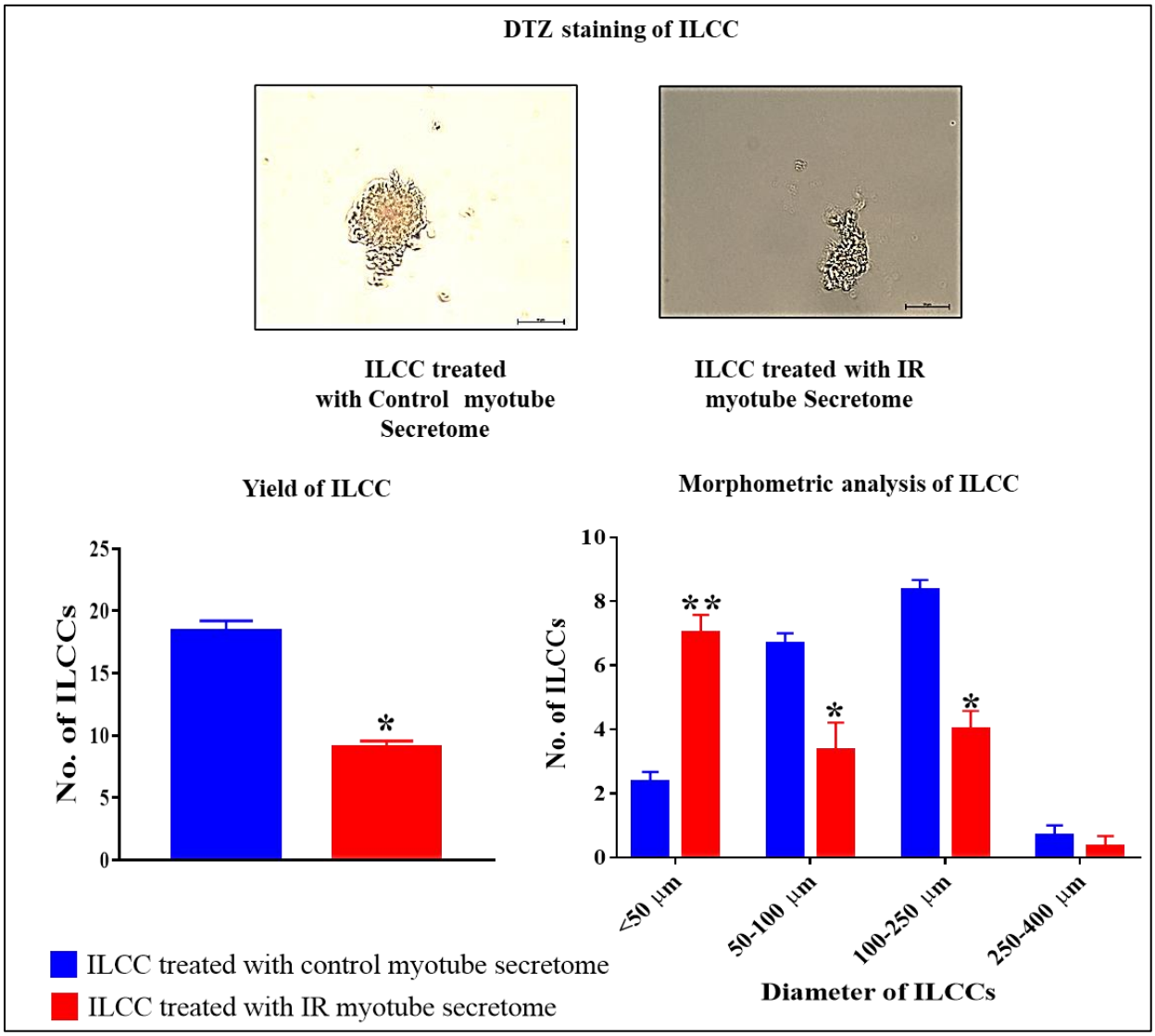

Figure 4.11 Functional analysis of ILCCs under the influence of C2C12 myotube secretome. PREPs were subjected to control and IR secretomes of C2C12 myotubes and ILCCs were differentiated. Functional parameters like DTZ staining (magnification 20X), Yield and Morphometric analysis was done. Data is expressed as Mean ± S.E.M. N=3. Significance is expressed as p-value *<0.05 ** <0.01

Chapter 4: Effect of secretome of skeletal muscle on islet differentiation & functionality

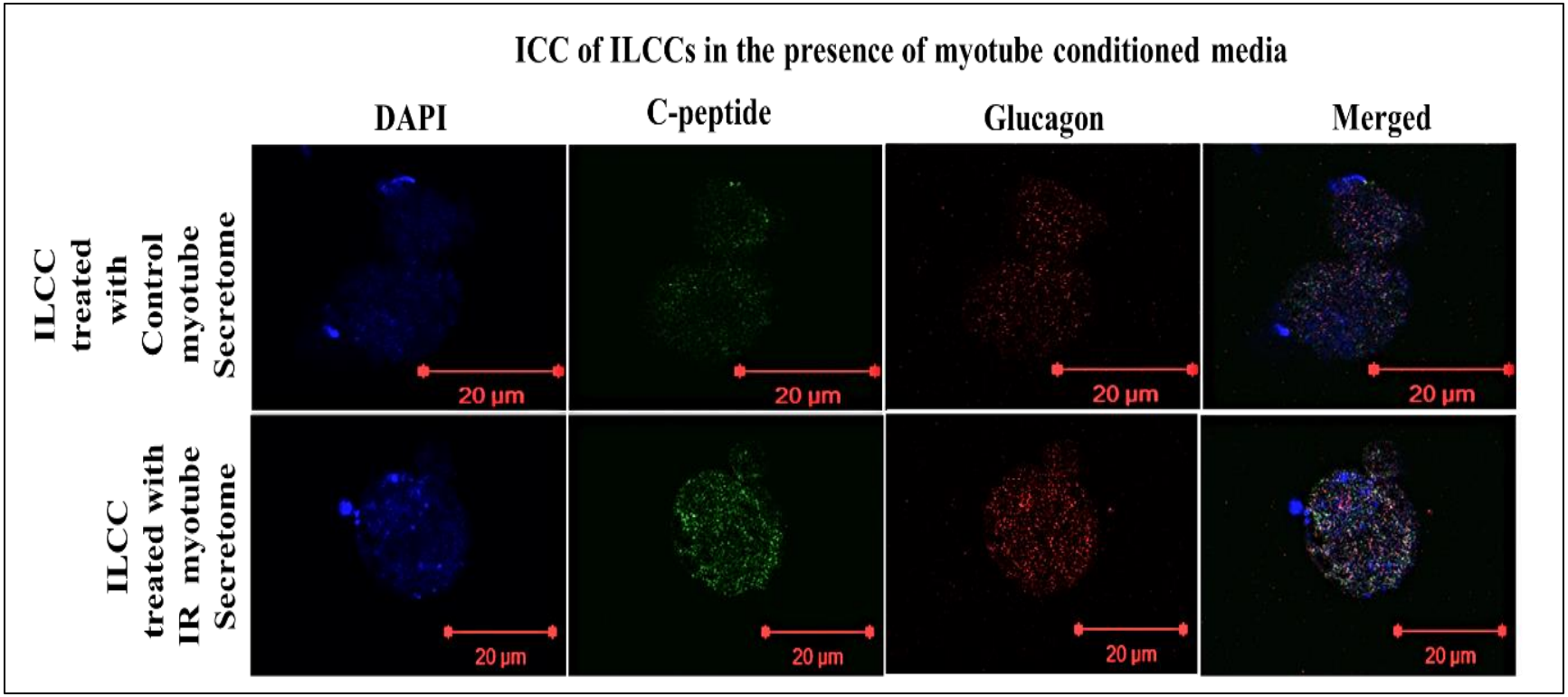

Figure 4.12 Functional analysis of ILCCs under the influence of C2C12 myotube secretome. Functional parameters like Immunocytochemistry of C-peptide and Glucagon were performed (magnification 63X).

4.3.6 ILCCs from PREPs under IR C2C12 myotube secretome demonstrate low islet cell survival and integrity

The discrepancies in islet functionality led our investigation to estimate the levels of intracellular ROS generation of ILCCs in both groups. So, DCFDA staining was performed (Fig 4.13) which showed higher intensity of green fluorescence in IR group depicting higher intracellular oxidative stress. ILCCs with low green intensity in control C2C12 myotube suggested cytoprotection against ROS generation.

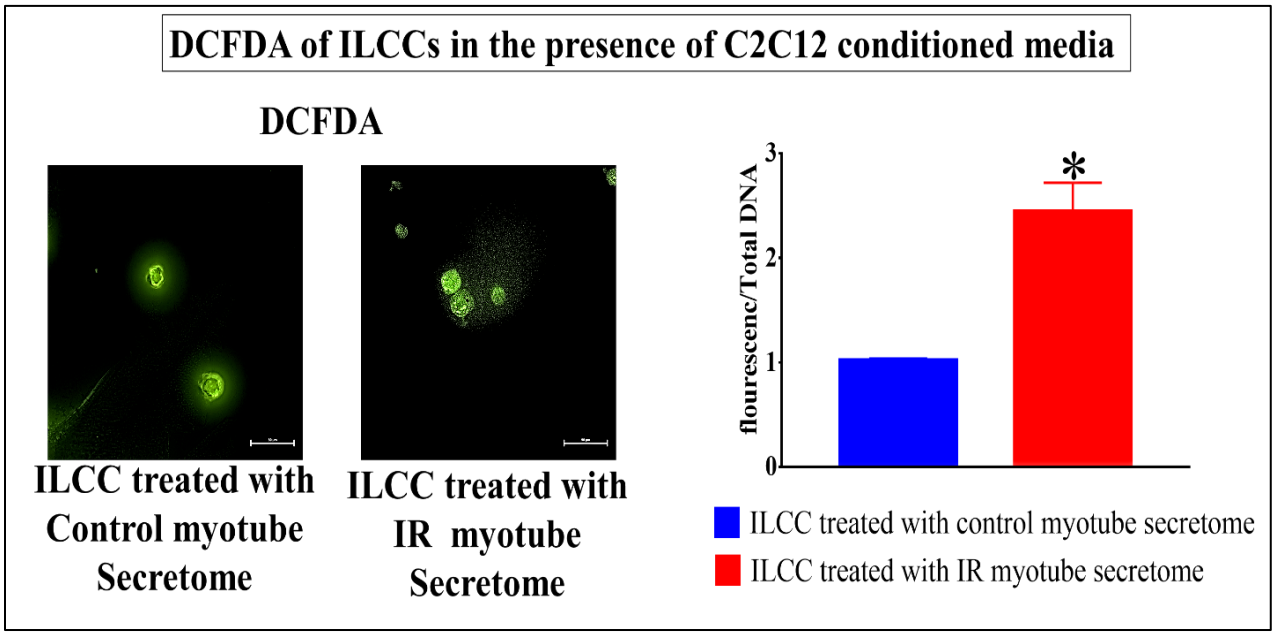

Figure 4.13 Islet integrity parameter of ILCCs under the influence of C2C12 myotube secretome was done. DCFDA analysis for ROS measurement was done. Data is expressed as Mean ± S.E.M. N=3. Significance is expressed as p-value *<0.05

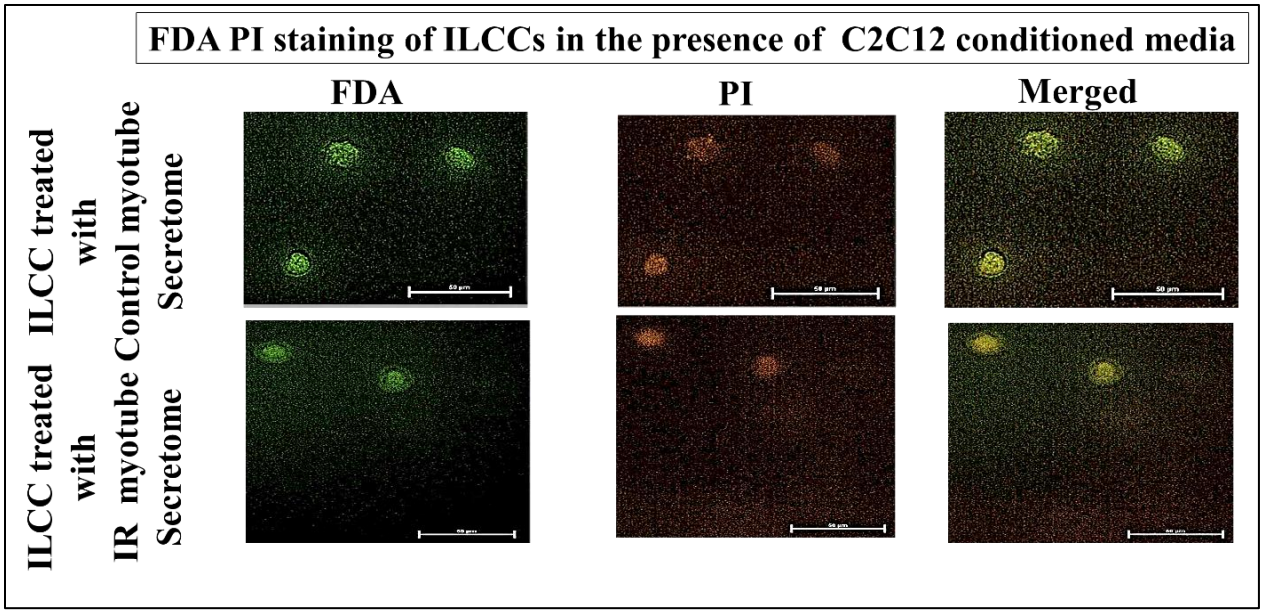

Figure 4.14 Islet survival parameter by FDA PI staining was performed (magnification 20X).

To substantiate further findings, we evaluated the viability of ILCCs by FDA/PI (Fig 4.14) and Annexin/PI stainings (Fig 4.15). ILCCs with control C2C12 myotube secretome were observed to have more green fluorescent intensity compared to IR which suggests more viable cells since FDA or Annexin stains live cells shown by green fluorescence. While dead cells are stained red by PI dye which were more evident in ILCCs with IR C2C12 myotube secretome.. This finding pointed towards the conviction of discordance of islet pathobiology under insulin resistance.

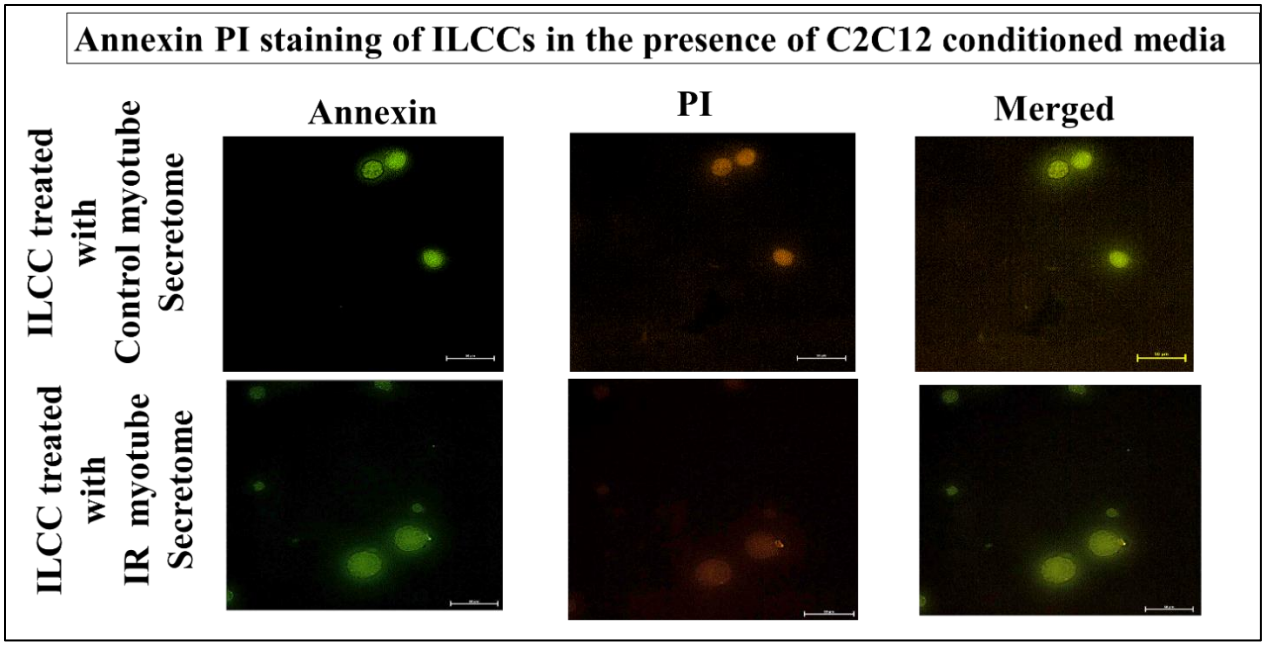

Figure 4.15 Islet survival parameter by Annexin PI was performed (magnification 20X).

Further cell death analysis was carried by monitoring Caspase-3 and Parp1 in a 4 day protocol of islet differentiation (Fig 4.16). We analyzed their expression on day 0, day 2, and day 4. Higher expression of both the markers were observed on day 4 indicating ascend of ILCCs into cell death. Densitometric analysis of PARP1 upregulation on day 4 in IR C2C12 myotube compared to day 4 control, suggesting its impact on differentiation and yield of viable and functional islet. This result substantiates the finding of detrimental effect on islet biology under different secretome conditions.

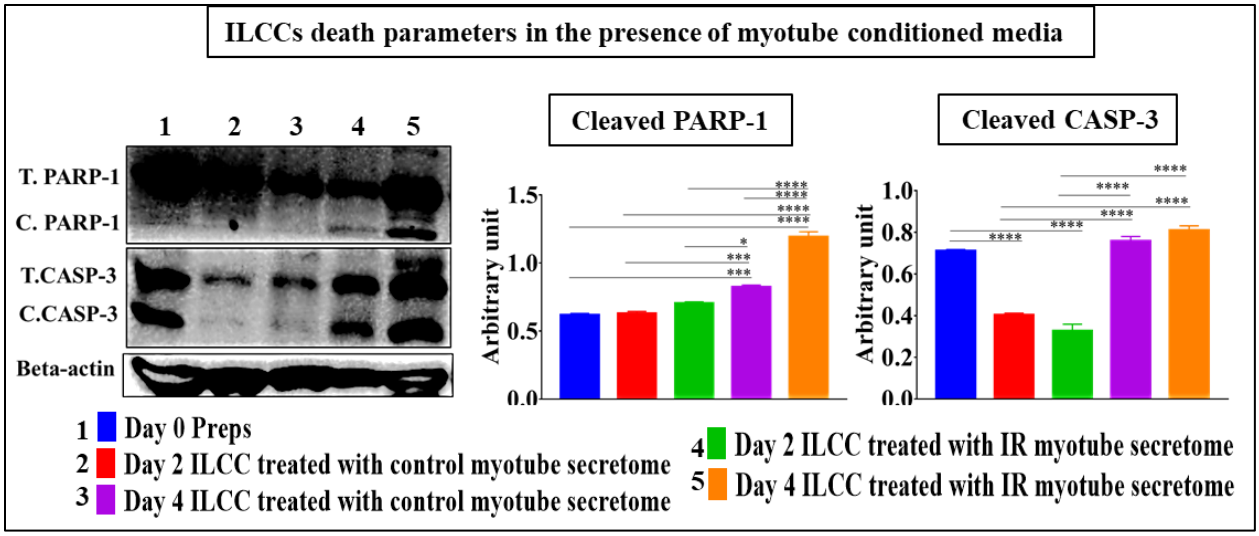

Figure 4.16 Western blotting of Parp1 and Caspase3 was done for cell death evaluation. Densitometric analysis of cleaved PARP-1 and CASP-3 was done normalized to Beta-actin and data expressed as arbitrary unit± S.E.M. N=3, Significance is expressed as p-value *<0.05, ** <0.01, * <0.001, **** <0.0001**

4.3.7 ILCCs from PREPs under control C2C12 myotube secretome demonstrates high fidelity towards differentiation

To understand the implications of the fate of islet differentiation at molecular level, we performed immunoblotting of key transcription factors which regulate islet differentiation at various stages. A series of a cascade of temporal transcriptional regulation propels pancreatic progenitors towards their inclination for islet differentiation. Stepwise differentiation of islet places FOXA2 or HNF-3B as a critical transcription factor. So, we analyzed the expression of FOXA2 or HNF-3B which plays a role in the development and is an important upregulator of PDX-1 which is redundant for pancreatic development (Lee, Cho et al. 2019). Expression increased on day 4 through day 2 in control but decreased on day 4 in IR group compared to day 2 IR. Next, we analyzed the master regulator NGN-3 (Zhu, Liu et al. 2017) which is a redundant marker of the progenitor state. The expression gradually increased on day 4 through day 2 in both groups. For NeuroD (Gu, Stein et al. 2010) expression gradually increased from day 2 to day 4 but expression decreased in IR group on day

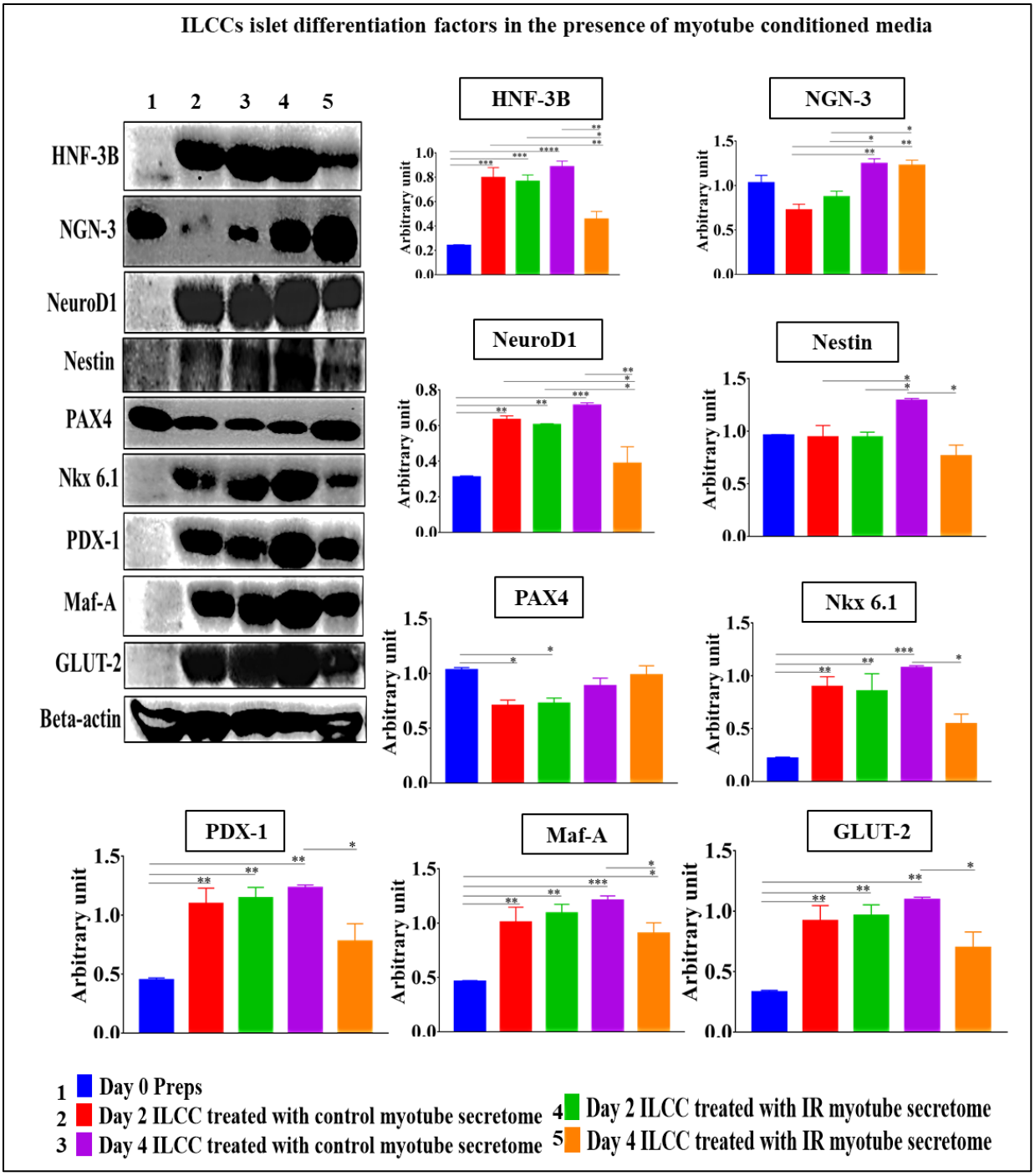

Figure 4.17 Temporal analysis of proteins involved in islet differentiation of ILCCs under the influence of C2C12 myotube secretome Differentiation of ILCC took place from day 0 to day 4 from PREPs with secretomes of C2C12 myotube. HNF-3B, NGN-3, Nestin, Pax4, Nkx6.1, NeuroD1, PDX-1, MaF-A and GLUT-2 expression was checked for islet

differentiation key proteins. Densitometric analysis was done normalized to Beta-actin and expressed as arbitrary unit± S.E.M. N=3, Significance is expressed as p-value *<0.05, ** <0.01, * <0.001, **** <0.0001**

4. Nestin positive cells serve as precursors of differentiated pancreatic endocrine cells (Hunziker and Stein 2000). Expression of Nestin increased on day 4 control but reduced in day 4 IR group. PAX4 is a key regulator of pancreatic islet development (Lorenzo, Fuente-Martín et al. 2015). Its expression decreased on day 2 compared to day 0 in both groups and non significant on day 4 compared to day 0 and 2. Nkx 6.1 increased on day 2 in both groups and eventually was higher in day 4 in control but decreased on day 4 in IR group.

Expression of PDX-1 and Maf-A (Nishimura, Takahashi et al. 2015) were increased on day 4 through day 2 but decreased on day 4 IR group. Finally, GLUT-2 (Thorens 2015) which is the most important glucose transporter, increased on day 2 and day 4 in control but decreased on day 4 in IR group (Fig 4.17).

This result strengthens the fact that islet differentiation was indeed altered by IR secretome in a detrimental manner lingering and delaying maturation and differentiation and thus yielding metabolically dysfunctional and sub-optimal islet like cell clusters.

4.4Discussion

Given a major insulin target tissue and an important site for post-prandial glucose disposal, skeletal muscle presents itself with challenges which culminate in cellular and systemic insulin resistance under a pathological condition like diabetes mellitus (DeFronzo and Tripathy 2009). Type 2 diabetes mellitus is characterized by a series of metabolic disturbances such as hyperinsulinaemia, increased hepatic gluconeogenesis, impaired glucose uptake, reduced secretion and regulation of incretin hormones, impaired mitochondrial capacity, endoplasmic reticulum stress, etc (Eckardt, Görgens et al. 2014) (Hameed, Masoodi et al. 2015).

The present study provides valuable insight on skeletal muscle-islet crosstalk under a normal and pathological condition like insulin resistance. The damaging effects of IR muscle secretome on islet functionality also give insights for detrimental effects on islet differentiation which is the noteworthy outcome of the present study. To understand the relationship between peripheral

insulin resistance of skeletal muscle and the progressive damaging effect on islet neogenesis, we studied the unexplored aspect of the influence of IR muscle secretome on islet differentiation.

We started with an established *in vitro* cell line model used for skeletal muscle and insulin resistance studies, C2C12 which are murine myoblast cells that differentiate into myotubes (Yaffe and Saxel 1977). Successful visualization of progressive fusion of myoblast into myotube was confirmed (Burattini, Ferri et al. 2004). By staining and higher expression of myogenic markers like myogenin, desmin, and αSMA. (Andrés and Walsh 1996) (Mermelstein, Amaral et al. 2005) (Corvino, Cerqua et al. 2021) (Springer, Ozawa et al. 2002).

Impaired insulin signaling is the principal feature of insulin resistance. Insulin resistance is a complex abnormality where insulin-sensitive tissue of the body becomes insensitive to the action of insulin. The contribution of TNFα has been closely associated with insulin resistance and inhibiting insulin secretion. In the present study *in vitro* insulin-resistant C2C12 skeletal muscle model was created by subjecting the myotubes to TNFα which is a key mediator of skeletal muscle catabolism and progressing inflammatory conditions. Dysregulation of key proteins of insulin signaling aggravates insulin resistance (Copps and White 2012). TNFα is known to mediate insulin resistance in skeletal muscle by downregulating IRS-1 and IR, key proteins of the Insulin signaling cascade. It inhibits tyrosine phosphorylation while producing serine phosphorylation of IRS-1 and IR in a p38 MAPK-dependent manner and impeding IRS-1-associated Akt activity (del Aguila, Claffey et al. 1999) (de Alvaro, Teruel et al. 2004). It is noteworthy that these effects were strongly observed in our study confirming development of IR model.

Far from being an inert organ, skeletal muscle actively takes part in interorgan communication by various secretory products which constitutes the secretome of the skeletal muscle. Various comprehensive quantitative analysis reports of skeletal muscle secretome points towards a wide range of secretory products including myokines (Goldstein 1961) (Pedersen and Febbraio 2012) (Whitham and Febbraio 2016).

Interleukin 6 which we found upregulated in IR condition in our study, has been identified as a prototype of the myokine which apart from its multifaceted actions, improve glucose tolerance by activating glucagon like peptide 1 (GLP1) in intestinal L cells and pancreatic islets to acclimatize insulin demand by enhancing insulin secretion and improving glycemia (Ellingsgaard, Hauselmann et al. 2011) (Pedersen and Febbraio 2012). Moreover, IL-6 released by contracting

skeletal muscle enhances the production of anti-inflammatory cytokines like IL-10, IL-1, IL-1RA, etc (Pedersen and Febbraio 2008). Of which IL-10 was downregulated in IR condition in our study, which is known to inhibit the production of proinflammatory factors such as IL-1α, IL-1β, TNFα, IL-8 and MIPα (Petersen and Pedersen 2005). IL13 and IL 15 are other two cytokines whose expression has been decreased in our study. Both these cytokines were found be decreased in type 2 diabetic patients (Rütti, Howald et al. 2016) (Al-Shukaili, Al-Ghafri et al. 2013). IL13 has a protective effect on islets by improving β cell survival against cytokine-induced apoptosis, without affecting glucose stimulated insulin secretion whereas IL-15 is identified as an anabolic factor (Grabstein, Eisenman et al. 1994) which plays an important role in the regulation of fat mass and muscle-adipose tissue interaction (Pedersen and Febbraio 2012) (Quinn, Anderson et al. 2009) thus exerts antiobesity effects by promoting lean body composition (Nielsen, Hojman et al. 2008). Pedersen et al demonstrated that Muscle-derived CXCL1 reduces diet-induced obesity through improvement of fatty acid oxidation and oxidative capacity in skeletal muscle tissue (Pedersen, Olsen et al. 2012) which was also downregulated in our study. Thus reduced expression of these cytokines in insulin resistant model can be well correlated with decreased islet functionality and obesity, major contributors of diabetes.

In contrast, CX3CL1 and FGF21 were found to be increased in the present study. Rutti et al demonstrated that human islets express and secrete CX3CL1 by imparting a protective effect on islets and decreases basal apoptosis of human β-cells It impacts islets by decreasing glucagon secretion without affecting insulin secretion (Rutti, Arous et al. 2014). FGF-21 is an insulin-regulated myokine, expressed in human skeletal muscle, improves glucose metabolism and insulin sensitivity. It is associated with chronic hyperinsulinemia (Hojman, Pedersen et al. 2009) and found to be increased in type 2 diabetic patients (Cheng, Zhu et al. 2011) thus correlated with present observations.

The secretome profile of skeletal muscle demonstrates a considerable change in insulin resistant condition with unfavorable effects on other tissues of the body including pancreatic islet β cells (Bouzakri, Plomgaard et al. 2011) (Ciaraldi, Ryan et al. 2016) Yoon et al have demonstrated relatively high similarity between the TNF-α induced secretome and the diabetic transcriptome of skeletal muscle (Yoon, Song et al. 2011). This supports the fact of differential expressions of proteins of TNF-α induced IR myotube secretome as observed in LCMS data of this study. The

secretome comprised of various proteins which were differentially expressed and regulated in control and IR C2C12 secretome. The majority of keratin proteins were overexpressed in IR C2C12 secretome compared to control. A reduced number of insulin vesicles are reported in pancreatic beta cells by targeting certain keratins leading to diabetes (Blessing, Rüther et al. 1993). Expression of Constitutive coactivator of peroxisome proliferator-activated receptor gamma was reduced in IR secretome. It is a constitutive co-activator PPARγ and promotes adipogenesis in a PPARγ-dependent manner (Li, Kang et al. 2007). PPAR-γ enhances glucose-sensing ability which helps in morphological and functional refurbishment of β-cells by TZDs (Kim and Ahn 2004). ECM collagen expansion is tightly associated with muscle IR. Collagens are the most abundant structural components of extra cellular matrix which is essential for cell adhesion and migration during growth and differentiation (Kang, Ayala et al. 2011). Reduced gene expression of several collagen types was found in streptozotocin-induced diabetic mice (Ahmad, Choi et al. 2020). We also observed reduced expression of collagen in IR secretome.

Classification of proteins under broad categories expands our knowledge of secretome discrepancies under insulin resistant conditions and its impact on islet differentiation and functionality were evaluated.

ILCCs formed under the effect of control C2C12 myotube secretome has been observed with more participation of PREPs, zone of activation and maximum cell aggregation towards cluster formation in contrast to IR. This compelling evidence of maturation of ILCCs was supported with enhanced expression of C peptide and glucagon, an unparalleled marker of islet functionality (Leighton, Sainsbury et al. 2017) Although the yield difference was insignificant, the morphometry analysis of ILCCs found abundance in range 100-150 um under control secretome and contrast to IR where most of the islet fall under 150-200 um (Bertera, Balamurugan et al. 2012) which reinstates the fact of compromised islet functionality in terms of morphometric characterization.

While evaluating ILCCs for cell death and integrity parameters, ILCCs with IR C2C12 myotube secretome had increased fluorescence staining imparted from DCFDA compared to control. This can be attributed to the fact of inherent lack of scavenging mechanism in a glucotoxic environment where generation of ROS is mostly observed (Bindokas, Kuznetsov et al. 2003) ILCCs demonstrated reduced differential staining of intact islets by Fluorescein diacetate/propidium iodide (FDA/PI) (Barnett, McGhee-Wilson et al. 2004). Plasma membrane integrity and

permeability is widely assed by Annexin V/ PI where apoptotic cells (Srivastava, Bhatt et al. 2016) were more prominent under IR C2C12 myotube secretome with distorted membrane integrity and progressive apoptosis with significantly high levels of PARP-1, DNA repair enzyme (Ko and Ren 2012) and Caspase 3, an apoptotic executor (Brentnall, Rodriguez-Menocal et al. 2013) signifying cell death. These observations emphasized the adverse effect of IR C2C12 myotube secretome on islet cell viability which highly limits the vital and morpho-functional abilities of the newly formed ILCCs. Bouzakri et al has observed increased apoptosis and decreased proliferation when subjected primary β-cells to conditioned medium from TNF-α-treated insulin-resistant myotubes as compared to control (Bouzakri, Plomgaard et al. 2011) co-relates with our results.

The marked observation that emerged from this study is the interaction between skeletal muscle and islets by trophic effects under normal and insulin resistance conditions on islet differentiation or neogenesis. The detrimental effects of IR muscle secretome on islet differentiation hamper the developmental and functional maturity of newly formed islets.

HNF-3B plays a crucial role in governing the morphogenesis of the pancreas. Lee et al. demonstrated that lack of HNF-3B in beta cells makes the mice hypoglycemic and dysregulates the insulin secretion (Lee, Sund et al. 2002). In our study, it is demonstrated that IR secretome causes a decrease in expression of HNF-3B on day 4 which causes dysregulated maturity of the newly formed islet. It is reported that the expression of NGN-3 along with pancreatic mesenchymal microenvironment are essential to promote pancreatic progenitors differentiated to islet cells (Yang, Wang et al. 2014) which was upregulated in both thegroups.

NeuroD is decreased in IR secretome compared to control on day 4. NeuroD is vital for proper activation of the transcriptional network and differentiation of functional α and β cells (Bohuslavova, Smolik et al. 2021) and it also sustains the functional identity of beta cells (Gu, Stein et al. 2010).Nestin which was found to be decreased on day 4 IR group has been reported by Lechner et al that nestin-positive islet-derived progenitor cells are a potential source of adult pluripotent stem/progenitor cells (Lechner, Leech et al. 2002).

PAX4 expression decreased on day 2 without any change on day 4. PAX4 states an expandable β-cell sub population within islets (Lorenzo, Fuente-Martín et al. 2015). It also promotes dedifferentiation and proliferation of β-cells through MafA suppression (Hu He, Lorenzo et al. 2011). Nkx 6.1 was higher on day 4 control but decreased on day 4 IR. Nkx 6.1 is an important

regulator of pancreatic β cell development, proliferation, and identity (Aigha and Abdelalim 2020). Taylor et al also found reduced levels of Nkx6.1 in human type 2-diabetic beta cells which causes rapid onset of diabetes (Taylor, Liu et al. 2013). Expression of PDX-1 was increased on day 2 propelling ILCC towards differentiation but decreased on day 4 IR. Reduced expression of PDX1 in β cells induces glucose intolerance (Holland, Hale et al. 2002) and found to be compromised in β cells T2DM patients (Guo, Dai et al. 2013)..

Maf-A expression was decreased on day 4 IR. Nishimura et al reported MafA is required for the maturity beta cells and its loss leads to loss of cell identity (Nishimura, Takahashi et al. 2015). Finally, GLUT-2 (Thorens 2015) expression was decreased on day 4 in IR group.Thus GLUT-2 was less expressed in islets when subjected to IR secretome which is the major glucose transporter in pancreatic β-cells (Wu, Fritz et al. 1998).

Thus the majority of a transcription factor for islet neogenesis is negatively regulated by insulin resistance suggesting a detrimental effect on islet neogenesis leading to morphologically and functionally compromised islets with increased oxidative stress and apoptotic markers.

Thus, this study gives an account of crosstalk of skeletal muscle and islets which widens the understanding of secretome therapeutics and investigates islet functionality and differentiation under pathological state.

4.5 Summary

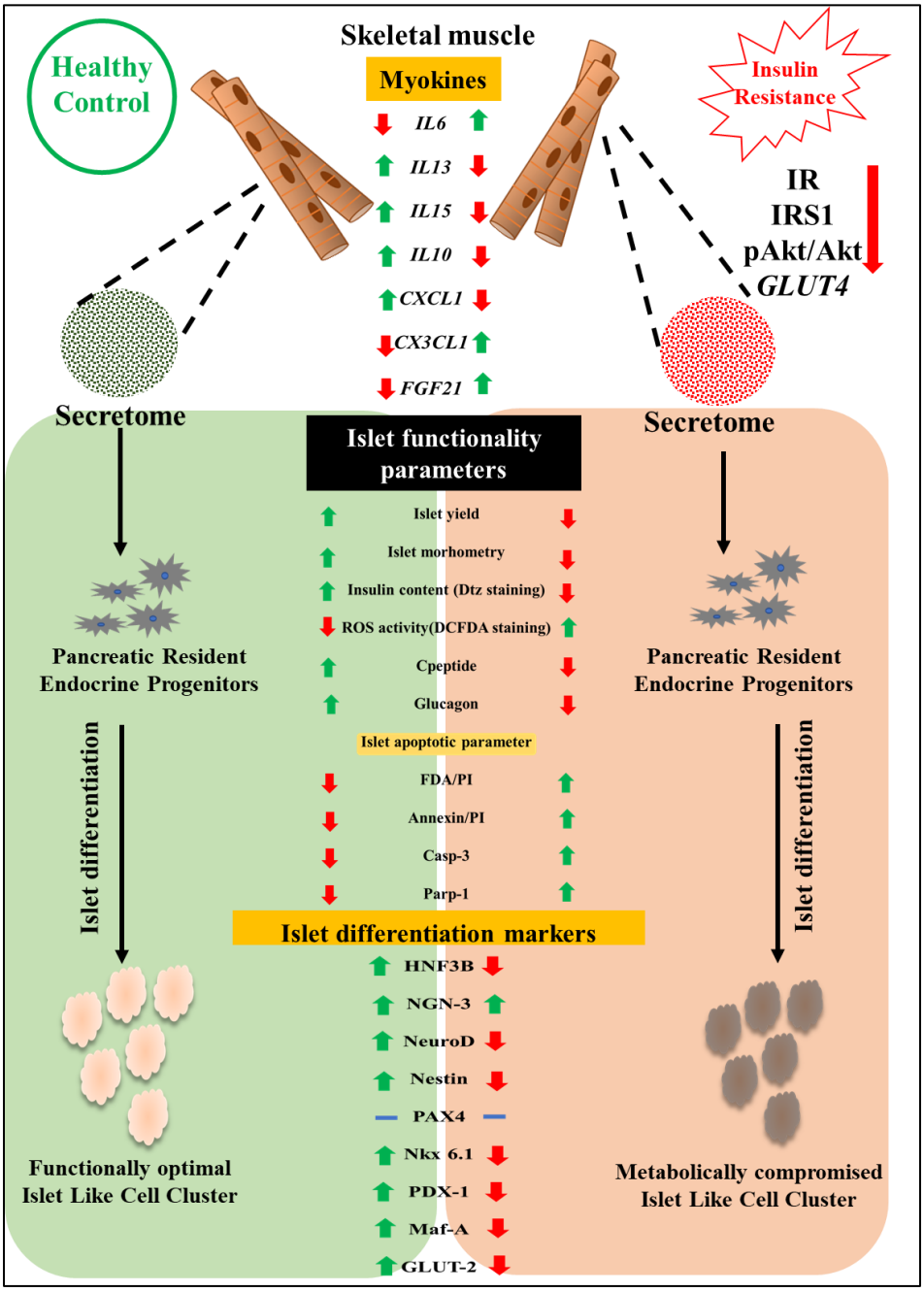

Figure 4.18 Summary of Chapter 4

Optimum regulation of metabolic activities is maintained by complex regulatory systems that contribute to various multifunctional cell communication in higher organisms. Such organ crosstalk is maintained by several secretory products that form an important component of the

process. Given the largest organ for glucose disposal and primary defect site for insulin resistance, skeletal muscle communicates differently with pancreatic islets which determines the vitality and functionality of the islets under a normal and pathological condition like insulin resistance. The present study emphasizes the potential role of healthy muscle secretome and progressive damage of islet under insulin resistance muscle secretome , not only in terms of islet functionality but also differentiation or neogenesis. This expands our understanding on muscle-islet crosstalk and great therapeutic potential of muscle secretome (Fig 4.18).